JOURNAL OF CATALYSIS 93, 176–181 (1985)

Zeolitic Diffusivities of Hydrocarbons by the Frequency Response Method

YUSUKE YASUDA[1] AND AKEMI YAMAMOTO

Faculty of Science, Toyama University, Toyama 930, Japan

Received June 15, 1984; revised November 29, 1984

In order to prove the efficiency of the new frequency response method by actual data, it is applied to propane and ethane over Linde 5A systems, in which considerable discrepancies remain unresolved between the diffusivities determined by the sorption and nuclear magnetic resonance (NMR) methods. The frequency response measurements of the systems reveal that both systems are composed of *two* types of intracrystalline diffusion processes whose Fickian diffusivities differ from each other four orders of magnitude; the large diffusivity agrees with that obtained from NMR experiments, whereas the small diffusivity corresponds to none of the diffusivities by standard methods. Based on the present results, a model of the zeolitic diffusion which contains two kinds of admolecules, tightly and loosely bound within the cages, is proposed. The frequency response method would be effective therefore to clarify the *whole* aspect of the kinetic phenomena which seems available to characterize zeolite catalysts.

INTRODUCTION

The small uniform pores and large intracrystalline volumes characteristic of zeolites make them ideally suited for shape-selective catalyst support (*1*). The intracrystalline diffusion coefficient of a gas is therefore a fundamental quantity to characterize the micropores and/or intracrystalline volumes.

The diffusion coefficient of a gas has usually been determined by matching experimental sorption curves to appropriate solution of a diffusion equation (*2, 3*). The NMR-pulsed field gradient technique, on the other hand, has been shown to be effective to determine the coefficients of hydrocarbons (*4, 5*). However, large discrepancies exist between the results by the two methods (*4, 6*). Though the discrepancies have been reduced in some cases for conjugated NMR and sorption experiments on the same (homemade) samples of large crystal size, they remain unresolved for commercial molecular sieves such as Linde 5A of smaller crystal size (*6*).

In a previous paper one of the authors proposed a frequency response (FR) method of determination of zeolitic diffusion coefficients (*7*) and the method has successfully been applied to Kr and Xe over Linde 5A systems (*8*). It seems of interest to apply it further to a hydrocarbon/Linde 5A system and to compare the result with those previously obtained by the standard methods.

EXPERIMENTAL

Apparatus. The FR apparatus was almost the same as that described elsewhere (*9*); the mean volume of the sorption chamber, V_c, was 1.145 and 1.120 dm^3 when the sorbent was maintained at (T_c =) 273 and 366 K, respectively; the relative amplitude of the sinusoidal volume variation, v, was 2.20×10^{-2} (at 273 K) or 2.23×10^{-2} (at 366 K) in standard runs.

Sorbent. Commercial synthetic 5A zeolites, Linde 5A (binder free), were used as sorbent. The powders pelletized were dehydrated at 383 K for 10 h. The temperature was raised to 673 K and evacuated at that level for at least 30 h. The amount of the

[1] To whom all correspondence should be addressed.

0021-9517/85 $3.00

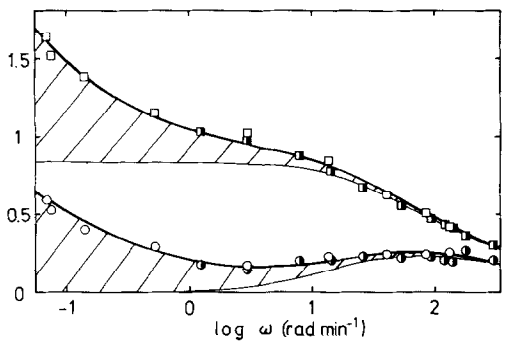

FIG. 1. Frequency response of the propane/Linde 5A system at T_e = 273 K and P_e = 9 Torr vs the angular velocity ω: (□ and ◨) in-phase component of $(v/p)\cos\varphi - 1$; (○ and ◑) out-of-phase component of $(v/p)\sin\varphi$; where (□, ○) and (◨, ◑) are the results measured at P_e = 8.8 and 9.2 Torr, respectively. The heavy solid curves are calculated from Eqs. (4) and (5); the light solid curves indicate contribution of the first terms and the shaded areas contribution of the second terms.

sorbent after these dehydrations was 9.87 g.

Sorbate. Tank propane (98 mol%; impurities were 1.3 mol% of C_2H_6, 0.7 mol% of i-C_4H_{10}, and 0.4 mol% of C_4H_{10}) or ethane (>99.9 mol%) was used as the sorbate.

RESULTS

In-phase and out-of-phase components, $(v/p)\cos\varphi - 1$ and $(v/p)\sin\varphi$, respectively, are plotted versus ω in Fig. 1, where p denotes the relative amplitude of the pressure variation induced, φ is the phase lag between the volume and pressure variations, and ω is the angular velocity of the sinusoidal waves. The periods of the oscillations corresponding to the largest and smallest ω's in Fig. 1 were 1.2 s and 1.5 h, respectively. Every component is the average value of at least four periods.

According to the theoretical procedure (*7*), the components may be described by

$$(v/p)\cos\varphi - 1 = \sum_n K_n \bar{\delta}_{3c}^{(n)} \qquad (1)$$

$$(v/p)\sin\varphi = \sum_n K_n \bar{\delta}_{3s}^{(n)}, \qquad (2)$$

where $\bar{\delta}_{3c}$ and $\bar{\delta}_{3s}$ denote the characteristic functions modified by a crystal-size distribution. It is found that, on the basis of the results obtained from the Kr/Linde 5A system (*8*), the functions can explicitly be given in the present case by

$$\bar{\delta}_{3j}^{(n)} = \frac{1}{(2\pi)^{1/2}\sigma} \int_0^\infty \delta_{3j} \left(\frac{D_n}{a_x^2}\right) \exp\left\{-\frac{(a_x - a_m)^2}{2\sigma^2}\right\} da_x \qquad (j = \text{c or s}), \quad (3)$$

where the standard deviation relative to the mean radius a_m, σ/a_m, was 0.5 (various defects in the crystal which have been observed with high-resolution electron microscopy (*10*) could have effectively been considered in this value besides the apparent value of 0.3–0.4 by a photomicrographic technique (*11*)); the explicit formulas of the characteristic functions, δ_{3c} and δ_{3s}, based on an isotropic sphere model are given elsewhere (*7, 8*). It should be noted that δ_{3s} (and then $\bar{\delta}_{3s}$) as a function of ω has a single peak and that δ_{3c} (and then $\bar{\delta}_{3c}$) tends to unity as $\omega \to 0$.

Since the results in Fig. 1 evidently reveal more than one peak in the out-of-phase components, two kinds of diffusion processes are assumed here. The heavy solid curves represent the theoretical results calculated from

$$(v/p)\cos\varphi - 1 = K_1\bar{\delta}_{3c}^{(1)} + K_2\bar{\delta}_{3c}^{(2)} \qquad (4)$$

$$(v/p)\sin\varphi = K_1\bar{\delta}_{3s}^{(1)} + K_2\bar{\delta}_{3s}^{(2)}, \qquad (5)$$

where the values of the four parameters, K_1, K_2, $\tilde{D}_1(= D_1/a_m^2)$, and $\tilde{D}_2(= D_2/a_m^2)$, given in Table 1, were determined as follows. The asymptotic value of the in-phase component in a lower ω region, $K_1 + K_2$, must be proportional to the gradient of the equilibrium isotherm (*7*):

$$K_1 + K_2 = \frac{RT_0}{V_e}\frac{d}{dP_e}(B_1 + B_2), \qquad (6)$$

where (RT_0/V_e) is the conversion factor and B_n denotes the amount of admolecules to

TABLE 1

Experimental Conditions and Concluded Values of the Parameters in Eqs. (4) and (5)

Exp. No.	P_e Torr	M^a	N^b	log ω^c	$\tilde{D}_1$ min^{-1}	$\tilde{D}_2$ min^{-1}	K_1	K_2	$\Delta_c \times 10^{2d}$	$\Delta_s \times 10^{2e}$
(Propane)										
1	2.8	2.5	11	−0.3–2.4	7.54 (±0.05)	5.5(±0.5) × 10^{-5}	0.98 (±0.03)	12.0 (±1)	1.42	2.34
2	5.4	2.9	13	−0.8–2.5	5.85 (±0.05)	8.0(±0.5) × 10^{-5}	0.75 (±0.03)	6.5 (±0.5)	2.86	3.49
3	8.8	3.2	21	−1.2–2.5	5.35 (±0.03)	3.0(±0.5) × 10^{-4}	0.85 (±0.03)	4.2 (±0.3)	2.99	2.31
4	9.2	3.2								
5	16.3	4.1	11	0.1–2.5	4.85 (±0.05)	1.2(±0.5) × 10^{-3}	0.74 (±0.03)	1.2 (±0.3)	2.64	2.36
(Ethane)										
6	5.2	0.6	11	−1.1–2.5	2.10 (±0.05)	3.8(±0.5) × 10^{-3}	4.74 (±0.03)	6.25 (±0.2)	5.75	15.0

[a] The number of molecules in a cage.

[b] The number of scans at different ω.

[c] The range of ω covered.

[d] The mean deviation of in-phase component defined by $\Delta_c = (1/N) \sum_i |\text{obsd} - \text{calcd}|$.

[e] The mean deviation of out-of-phase component defined by $\Delta_s = (1/N) \sum_i |\text{obsd} - \text{calcd}|$.

which K_n and D_n are attributable. Therefore, the sum of $K_1 + K_2$ can be predicted from the gradient of the isotherm. On the other hand, the height of the out-of-phase component in the higher ω region in Fig. 1 would approximately be 0.27 K_1 (*8*). The most probable values of the parameters in Table 1 were determined after repeated calculation by a computer for various choices of them around the initial values thus estimated. Contribution of the first terms is represented by the light solid curves and that of the second terms is indicated by the shaded areas.

The experiments were repeated at different equilibrium pressures. The values of the parameters determined by the computer simulation are summarized in Table 1 and plotted in Fig. 2 as functions of the equilibrium pressure.

The nearly constant K_1 means that B_1 is almost proportional to P_e so that B_1 species would be loosely bound. On the other hand, the sudden decrease in K_2 with increasing P_e indicates the saturation of B_2 at the higher pressure or tightly bound B_2 species. The ratio B_1/B_2 could be derived from the pressure dependence and found to be 0.1 at P_e = 9 Torr (1 Torr = 133.3 Pa) of Fig. 1, when total amounts of admolecules, $B_1 + B_2$, were 1.9 mmol/g or 3.2 molecules/cage.

In contrast with the case of Kr or Xe/

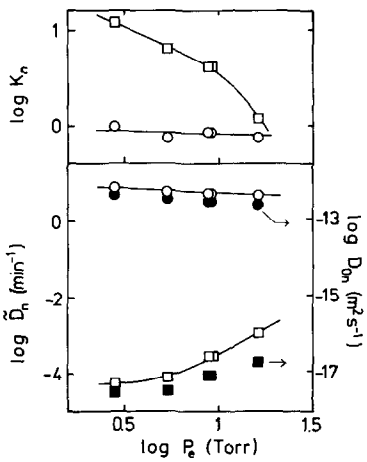

FIG. 2. Plots of the parameters in Table 1 as functions of P_e: all circles refer to n = 1; all squares to n = 2. Solid symbols are the corrected diffusivities derived from the parameters.

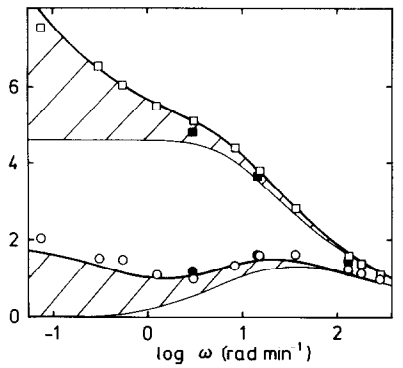

FIG. 3. Frequency response of the ethane/Linde 5A system at T_c = 273 K and P_e = 5.2 Torr vs the angular velocity ω: (□, ○) with $v = 2.23 \times 10^{-2}$; (■, ●) with $v = 5.03 \times 10^{-2}$. Notation is that of Fig. 1.

Linde 5A (*8*), two kinds of admolecules are required in the data analysis. In order to confirm the unexpected results, additional experiments with ethane of adequate purity instead of propane were carried out. The results are plotted in Fig. 3; the solid curves represent the computed results with the parameters given in Table 1. It is noted that K_1 is comparable to K_2 in this case in contrast with the case of propane ($K_1 \ll K_2$). In the course of the experiments, v was increased from 2.23×10^{-2} to 5.03×10^{-2}. However, the FR data were practically unaltered as shown in Fig. 3. It may be concluded therefore that effects of both heat and mass transfer resistance (*12*) are negligible in the present work.

Typical data of propane observed at a higher equilibrium temperature, 366 K, are shown in Fig. 4, in which total amount of admolecules was 0.27 mmol/g or 0.4 molecules/cage; the asymptotic value of the in-phase component obtained from the gradient of the isotherm was 4.0. Evidently, it is impossible for them to be described by Eqs. (1) and (2) because the in-phase components are smaller than the out-of-phase components in the higher ω region. This means that Fick's law is inadequate in this case. It should be noted however that there appear two peaks of comparable heights in the out-of-phase components and that the amount of B_1 species at 366 K would be larger than that at 273 K at an equilibrium pressure around 5 Torr because the first peak was higher than that of Fig. 1.

DISCUSSION

The Fickian diffusivities D_1 and D_2 can be evaluated from $\tilde{D}_1$ and $\tilde{D}_2$ provided $a_m = 1.8$ μm (*11*) and the corrected diffusivities based on a chemical potential driving force (*13*), D_{01} and D_{02}, could be given by

$$D_n = D_{0n}\left(\frac{\partial \ln P_e}{\partial \ln B_n}\right)_T \qquad (7)$$

provided the *individual* isotherm $B_n(P_e)$ are derived from the P_e dependence of K_n. The results are shown by the solid symbols in Fig. 2. They are compared further with the values determined by the NMR and sorption techniques (*6*) in Fig. 5. The fast diffusivity would correspond to the results by the NMR method because it agrees with the value on the dashed line extrapolated (identical activation energy was obtained from diffusivities by NMR and sorption experiments in the case of butane (*6*)).

Based on the experimental results, a model of the diffusion shown in Fig. 6 could be derived. The depth of the potential wells for B_2 species of propane is ca. 35 kJ/mol; this is the heat of absorption determined from the equilibrium isotherms by making use of Clausius–Clapeyron equation. The potential barrier for crossing the windows

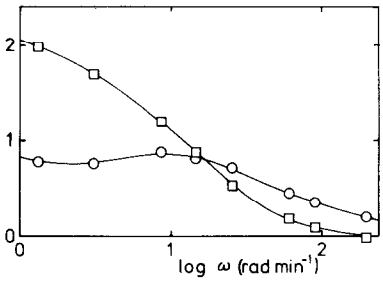

FIG. 4. Frequency response of the propane/Linde 5A system at T_c = 366 K and P_e = 8.9 Torr vs the angular velocity ω. Notation is that of Fig. 1 but the smoothed curves are temporarily drawn.

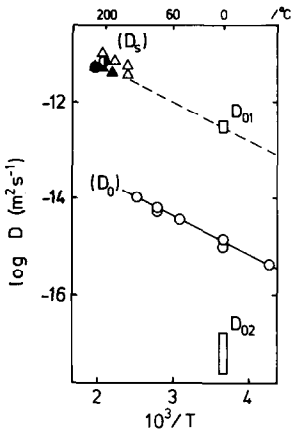

FIG. 5. Diffusivities of propane in zeolite 5A determined by different methods vs the equilibrium temperature T_e: the top and bottom of the rectangles indicate the maximum and minimum of the diffusivities by the FR method; (○) the diffusivities in Linde 5A by the sorption method (*6*); (△, ▲) and (◑, ●) are the diffusivities in zeolite 5A of large crystal sizes determined by the NMR and sorption methods, respectively (*6*).

is ca. 15 kJ/mol; this is the apparent activation energy of the solid and dashed lines in Fig. 5.

According to the model, a rough estimation of the temperature dependence of B_1/B_2 is possible:

$$\frac{B_1}{B_2} = \frac{q_1}{q_2} \exp\left\{-\left(\frac{35 - 15}{8.3 \times 10^{-3}}\right)/T_e\right\}, \quad (8)$$

where q_n denotes the partition function. Since B_1/B_2 was 0.1 at 273 K, q_1/q_2 is expected to be about 700. On the assumption of q_1/q_2 being constant, one finds that $B_1/B_2 = 1$ and 4 at 366 and 473 K, respectively. Consequently, B_1 species are probably dominant at the higher temperatures of Fig. 5 where the NMR experiments (and also the sorption experiments of large crystal sizes) were performed; the results by both NMR (D_s) and sorption techniques would necessarily correspond to D_{01}. The failure of the curve fitting the FR data at 366 K in Fig. 4 is perhaps due to the comparable amounts of B_1 and B_2 species or fast transition between them at the intermediate temperature.

The discrepancies between the values obtained from the FR and sorption experiments at a lower temperature could be explained as follows. The sorption measurements were usually performed at higher pressures, because reliable sorption diffusivities could not be obtained at low sorbate concentrations (*6*). Since B_2 species is expected to be nearly saturated at the high pressure, the amount of B_1 species alone would be affected by a (small) step change in the pressure. Consequently, B_2 species could not have been detected by the sorption method. On the other hand, the (small) step change is enormously larger than the change induced by the volume variation in the FR experiments and therefore the gradient of the concentration of sorbate would be considerably large at an entrance of the micropores. Dependence of the flux of sorbate j at the entrance upon the gradient dc/dx is shown in Fig. 7; in the

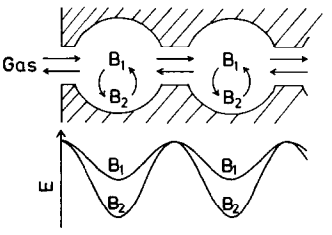

FIG. 6. Model of the zeolitic diffusion of propane: the upper side is schematic diagram of the diffusion in the micropores; the lower is the potential energy profiles for B_1 and B_2 species of propane absorbed. The depth of the potential wells for B_2 is ca. 35 kJ/mol and the barrier for B_1 to cross the window is ca. 15 kJ/mol.

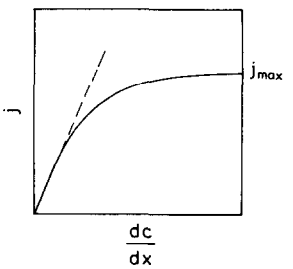

FIG. 7. Flux of molecules j at an entrance of micropores vs the gradient of concentration of sorbate at the entrance dc/dx.

small gradient region, j may be proportional to the gradient according to Fick's first law, while j would asymptotically reach the limit j_{max} with increasing gradient because of the finite size of the entrance. Consequently, the diffusivity by the sorption method should unavoidably be underestimated, though the activation energy would be unaltered irrespective of the saturation of the flux because only the potential barrier controls the diffusion process.

The remarkable increase in D_2 with increasing amounts of admolecules (from 2.5 to 4.1 molecules/cage) is probably attributed to repulsive forces between B_2 species or a finite number of minima in the potential energy; the saturation concentration at 273 K is expected to be 4.6 molecules/cage (*13*).

In the case of Xe molecules at 273 K (*8*), whose cross section is almost the same as that of *n*-paraffins, the FR data led to only one diffusion constant, while those of both propane and ethane reveal the two types. The fact supports the conclusion that the two types of diffusion processes can be expressed in terms of the two kinds of admolecules rather than inter- and intracrystalline diffusions. Potential energy profiles for a xenon atom in an idealized 5A zeolite cavity have been calculated and two potential minima of 33 and 25 kJ/mol are concluded (*14*).

Since intracrystalline volumes as well as micropores would affect the activity and/or selectivity of zeolite catalyst, it seems of interest to study the effects of various modifications of the catalyst upon each of the diffusion processes individually; modifications such as dehydration, cation exchange, preadsorption of a gas, deactivation by a reaction, and so on. The present method may be regarded as a *probe* for the micropores by means of *various* gases.

ACKNOWLEDGMENTS

The authors thank Mr. G. Sugasawa for help in the measurements. This work was supported in part by a Grant for Fundamental Research in Chemistry, Japan Society for the Promotion of Science.

REFERENCES

1. Csicsery, S. M., *in* "Zeolite Chemistry and Catalysis" (J. A. Rabo, Ed.), ACS Monograph 171, p. 680. Amer. Chem. Soc., Washington, D.C., 1976.
2. Breck, D. W., "Zeolite Molecular Sieves." Wiley, New York, 1974.
3. Eberly, P. E., Jr., *in* "Zeolite Chemistry and Catalysis" (J. A. Rabo, Ed.), ACS Monograph 171, p. 392. Amer. Chem. Soc., Washington, D.C., 1976.
4. Kärger, J., and Caro, J., *J. Chem. Soc. Faraday I* **73,** 1363 (1977).
5. Kärger, J., Pfeifer, H., Rauscher, M., and Walter, A., *J. Chem. Soc. Faraday I* **76,** 717 (1980).
6. Kärger, J., and Ruthven, D. M., *J. Chem. Soc. Faraday I* **77,** 1485 (1981).
7. Yasuda, Y., *J. Phys. Chem.* **86,** 1913 (1982).
8. Yasuda, Y., and Sugasawa, G., *J. Catal.* **88,** 530 (1984).
9. Yasuda, Y., and Sugasawa, G., *J. Phys. Chem.* **86,** 4786 (1982).
10. Bursill, L. A., Lodge, E. A., and Thomas, J. M., *Nature (London)* **286,** 111 (1980).
11. Loughlin, K. F., Derrah, R. I., and Ruthven, D. M., *Canad. J. Chem. Eng.* **49,** 66 (1971).
12. Yucel, H., and Ruthven, D. M., *J. Chem. Soc. Faraday I* **76,** 71 (1980).
13. Ruthven, D. M., and Loughlin, K. F., *Trans. Faraday Soc.* **67,** 1661 (1971).
14. Derrah, R. I., and Ruthven, D. M., *Canad. J. Chem.* **53,** 996 (1975).